N73-12143
USCEE Report 426

UNIVERSITY OF SOUTHERN CALIFORNIA

SYNCHRONIZATION USING PULSED EDGE TRACKING IN OPTICAL PPM COMMUNICATION SYSTEMS

R. Gagliardi

Interim Technical Report

September 1972

This work was sponsored by the National Aeronautics and Space Administration, under NASA Contract NGR-05-018-104. This grant is part of the research program at NASA's Goddard Space Flight Center, Greenbelt, Maryland.

ELECTRONIC SCIENCES LABORATORY

USC Engineering

USCEE Report 426

September 1972

Synchronization Using Pulsed Edge Tracking in Optical PPM Communication Systems

R. Gagliardi

Interim Technical Report

Department of Electrical Engineering
University of Southern California
Los Angeles, California 90007

This work was sponsored by the National Aeronautics and Space Administration, under NASA Contract NGR-05-018-104. This grant is part of the research program at NASA's Goddard Space Flight Center, Greenbelt, Maryland.

ABSTRACT

A pulse position modulated (PPM) optical communication system using narrow pulses of light for data transmission requires accurate time synchronization between transmitter and receiver. The presence of signal energy in the form of optical pulses suggests the use of a pulse edge tracking method of maintaining the necessary timing. In this report the edge tracking operation in a binary PPM system is examined, taking into account the quantum nature of the optical transmissions. Consideration is given first to "pure" synchronization using a periodic pulsed intensity, then extended to the case where position modulation is present and auxiliary bit decisioning is needed to aid the tracking operation. Performance analysis is made in terms of timing error and its associated statistics. Timing error variances are shown as a function of system signal to noise ratio.

1.0 Introduction

The successful operation of any digital communication system requires accurate time synchronization between the transmitter and receiver. In optical digital systems a common procedure is to use a noncoherent pulse position modulation (PPM) mode of operation using narrow pulses of light intensity to carry the data [1]. The presence of signal energy in the form of optical pulses suggests the use of a pulse-edge tracking method of maintaining the necessary time synchronization. In pulse edge tracking the edges of the transmitted pulses are used as timing markers to adjust the synchronization of the receiver. When the optical pulses are transmitted as a periodic pulse train of known fixed frequency, the edge tracking corresponds to "pure" synchronization, in that the transmitted edges always occur at periodic points in time. When position modulation is present, however, the pulses of light are shifted according to the data, and the edge tracking operation must be modified in order to maintain receiver timing. The latter type of synchronization is often called modulation-derived synchronization, or "impure" syncing, since the timing must be derived from, or accomplished in the presence of, the data modulation. In this report we examine the pure and impure edge tracking operation in an optical binary PPM system, taking into account the quantum nature of the light transmission. Performance comparisons are made in terms of the instantaneous timing error of the receiver and its associated statistics. The effect of imperfect timing on the overall data decoding operation has been studied elsewhere [2] and will not be considered here. In addition, it will be assumed that initial acquisition of beam and waveform has already been achieved, and only

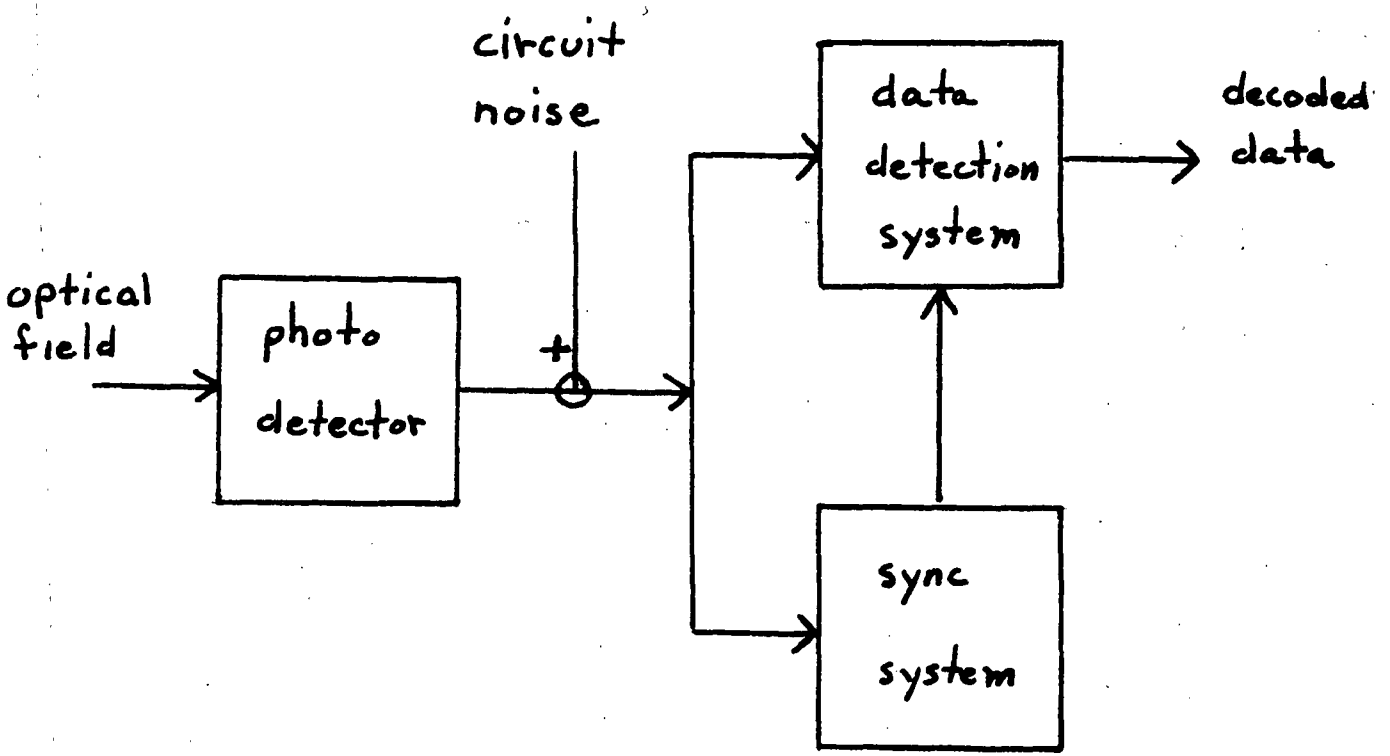
circuit
noise
data
detection
system
decoded
data
optical
field
photo
detector
+
sync
system

Figure 1

the maintainance of continuous time synchronization will be investigated.

2.0 System Description

A block diagram of an optical digital system is shown in Figure 1. In normal operation the incident optical field is photo detected, and the recovered signal is processed in both a data detection channel and in a synchronization channel, the latter providing the timing for the former. In this report only the synchronization subsystem will be considered. In a PPM non-coherent mode of operation, digital information is transmitted by position modulating pulse of light intensity during each data bit interval. Thus, in a binary system, the light energy is transmitted in one of two adjacent bit subintervals, representing a binary one or binary zero, as shown in Figure 2a. Detection in the data channel is made by photo electron counting (physically, short term integration of the photo detector output, which is equivalent to energy detection of the optical field) during each subinterval, deciding on the position with the highest count as containing the transmitted bit. Timing for the starting and stopping of each counting interval is provided by the synchronization subsystem, and timing errors (offsets between received and integrating bit intervals) lead directly to system degradation. Continual timing in a digital system is necessary to maintain bit timing in spite of the time delay variations that may occur during optical transmission, (i.e., the received waveform and associated timing markers are unintentionally varied from their expected position).

The system of Figure 1 can operate with one of two different synchronization formats. For pure sync operation, an unmodulated sync signal (herein

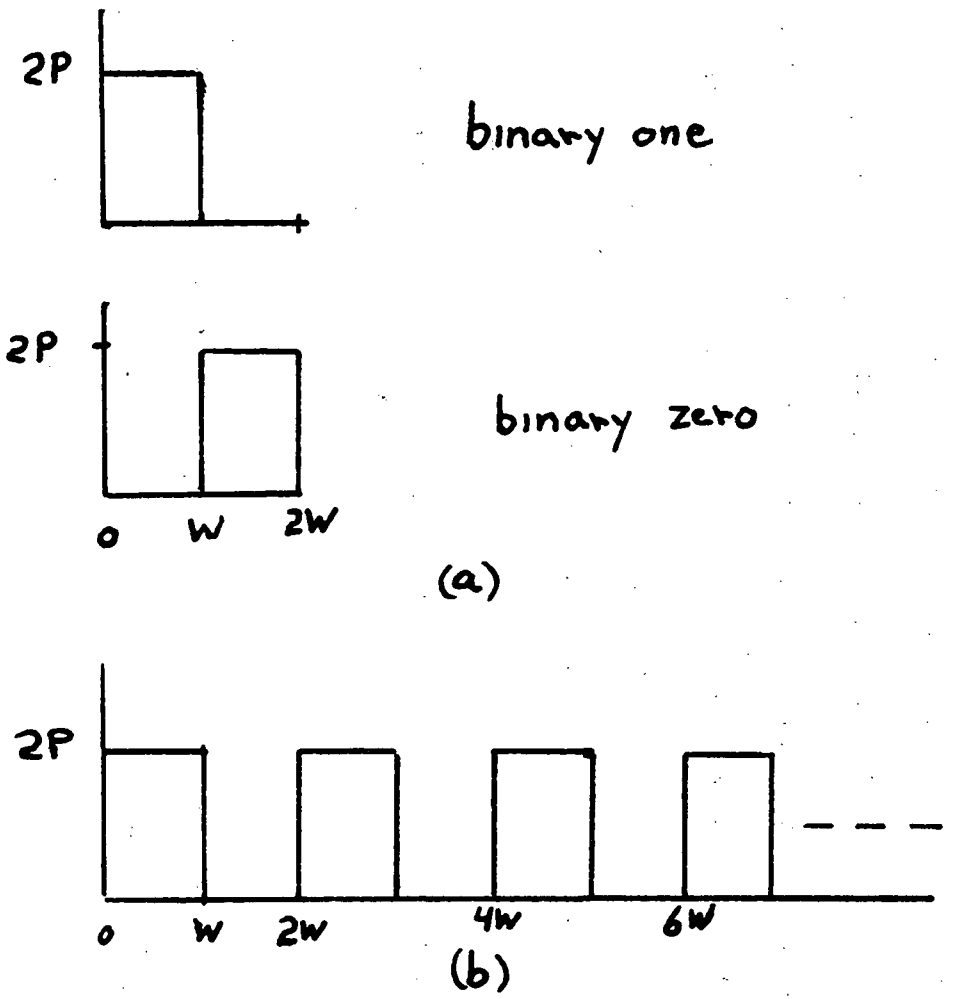

Figure 2

considered as a periodic train of optical pulses at the bit rate frequency), shown in Figure 2b, is transmitted intermittantly in place of the data to allow receiver lock up, and the resulting timing is used to decode the subsequent data transmissions until the system is retimed with the next sync burst. In impure sync generation, the PPM data is transmitted continuously and the timing is extracted from the data. The first procedure allows pure synchronization but must sacrafice data during the timing operation. The second method allows uninterrupted data transmission, and is obviously the preferred method of operation, but requires modulation-derived synchronization. For this reason considerable interest exists in developing the latter system, and to determine the achievable performance with impure synchronization.

In pulsed optical systems both the pure and impure sync systems can employ edge-tracking for timing. An edge tracking subsystem makes use of the fact that a pulse edge always occurs at the center of each bit interval (see Figure 2) and can therefore be used to sync an identical pulse train at the receiver. The subsystem, to be described in Section 3 and 4, employs a feedback loop to essentially measure timing errors between the received and receiver edges, using the error to correct the latter signal. In pure synchronization the pulse edge at the center always corresponds to the trailing edge of a pulse. When PPM is present, however, the edge may represent either a leading or trailing edge, and this polarity must be determined for successful loop operation. To accomplish this, the modulation-derived sync subsystem employs an auxiliary decision-making

loop that operates in conjunction with the edge tracking loop [see Figure 7]. This auxiliary loop essentially decides which type of edge (i.e., which data bit) is being received, using the decision to augment a delayed version of the standard edge tracking loop. Similar systems have been previously proposed [3].

Continual or updated timing is necessary to overcome the unintentional variations in transmission delay, due to doppler, relative receiver motion, etc. If the basic assumption is made that these delay variations are slow relative to the optical pulse width, then their only effect is to vary the time location of the optical pulse without distorting its shape. Thus, if I(t) represents the pulsed light intensity at the receiver with no delay variations, and if τ_d is the time varying delay occurring, then the recovered field intensity is given by $I(t-\tau_d)$. Here it is tacitly implied that τ_d is a function of t that changes slowly with respect to the pulse width of I(t). Note this latter condition is equivalent to the assumption that the bandwidth of τ_d is much smaller than the bandwidth of I(t). The principle objective of the edge tracking loop is therefore to "track out" the unintentional time variations of τ_d generated during the transmission of the optical field.

3.0 Edge Tracking of a Periodic Pulse Train (Pure Sync)

In this section we first examine the edge tracking operation when the received intensity corresponds to a periodic pulse train of light. This would represent the situation during pure synchronization operation when the data modulation is not present (actually, a periodic pulse train at the bit frequency can be considered as a continuous sequence of the binary one

symbol in Figure 2a). The received field intensity with no delay variations is therefore given by

$$I(t) = P[1 + p(t)] \tag{1}$$

where P is the received field power per unit area, and p(t) is the effective intensity modulation

$$p(t) = \begin{cases} 1 & 0 \le t \le W \\ -1 & W \le t \le T \end{cases} \tag{2}$$

Here W is the pulse width and T = 2W is the bit period. The above intensity is assumed to be received with the delay variations τ_d, which is equivalent to replacing p(t) by $p(t-\tau_d)$.

The output of the photo-detector in Figure 1 , operating over a single spatial mode of the optical field, is known to be the shot noise current process [4]

$$i(t) = Ge \sum_{m=1}^{N(0,t)} \delta(t-t_m) \tag{3}$$

where $\delta(t)$ is the detector impulse function, e is the electron charge, G is the photomultiplication gain, $\{t_m\}$ are the random location variables, and N(0,t) is the electron poisson counting process [i.e., N(0,t) is the number of electrons occurring in the interval (0,t)]. The counting process has its average value related to the received field intensity, I(t), by

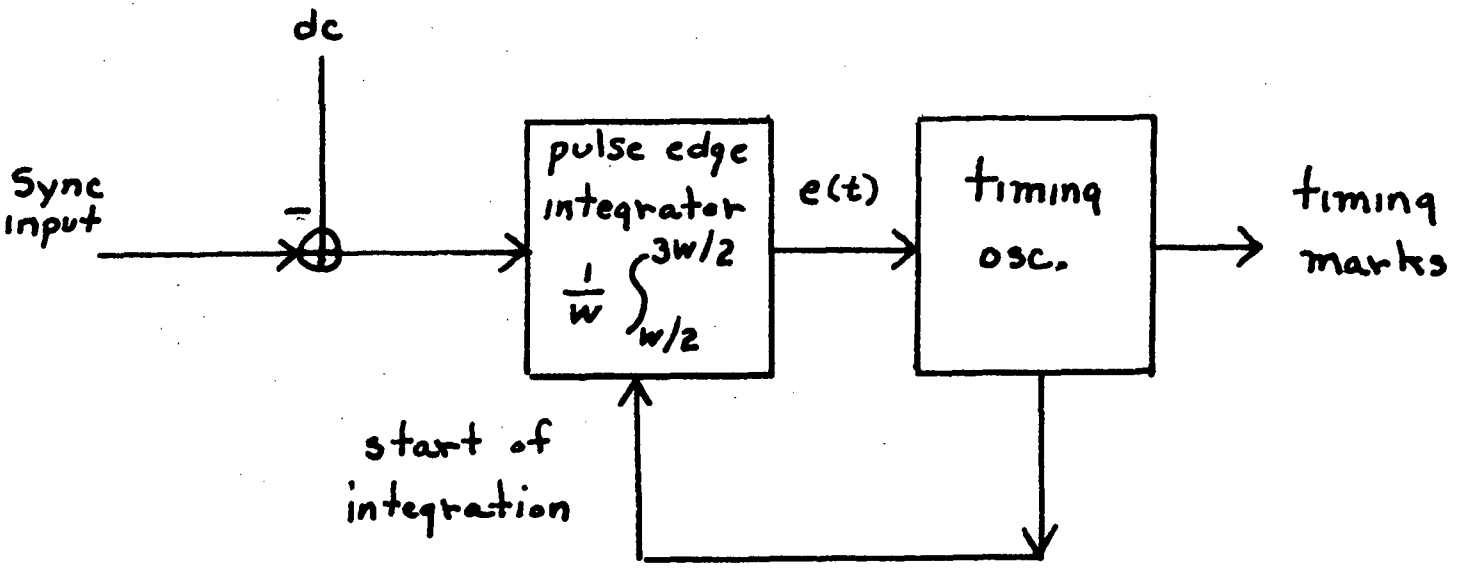
dc
Sync input
−
pulse edge integrator
$\frac{1}{w}\int_{w/2}^{3w/2}$
e(t)
timing osc.
timing marks
start of integration

Figure 3

$$\text{average } N(t_1, t_2) = \beta\left[\int_{t_1}^{t_2} I(t)dt + k_n\right] \qquad (4)$$

where $\beta = 1/hf$, a = detector area, h = Plancks constant, f is the optical frequency, and βk_n = average rate of noise background photons per detector area. The photodetector output i(t) of (3) will have added to it a white Gaussian circuit noise current $i_n(t)$, and the resulting signal, $x(t) \triangleq i(t) + i_n(t)$, provides the input to the synchronization edge tracking subsystem, shown in detail in Figure 3. A pulse-edge integrator is time controlled by a receiver timing oscillator, generating an error voltage used to readjust the oscillator. The latter, in addition, provides the timing markers for the data channel. The pulse-edge integrator consists of simply a W sec offset integration over the trailing edge of the received pulse. If the input to the integrator was the pulse train of Figure (2b) with zero average value (i.e., with its d.c. value removed) the offset integration occurs over portions of positive and negative values. If this latter integration had been timed to begin exactly half way through the positive pulse (at t = W/2), the resulting integrated error value would be zero, no oscillator correction is necessary, and the system is in time sync. If a time difference occurred between start of integration and pulse half interval point, a proportional timing error would be generated whose polarity depended on the direction of the time difference. This error voltage can be used to adjust the loop timing oscillator. The input d.c. removal can be accomplished easily by capacitor-coupled circuits, but is represented

as a subtraction in the mathematical model of Figure 3. Unfortunately, in the optical system of Figure 1, the input to the loop is not a clean pulse sync train, but rather the shot noise process of (3), containing the optically pulsed intensity of (1). In addition, this shot noise has added to it the additive circuit white noise current $i_n(t)$. Hence, the error signal generated after the short term loop integration is then

$$e(t) = \frac{1}{W}\int_{\tau_\ell}^{\tau_\ell+W} [i(t) + i_n(t) - Ge\beta(P+k_n)]dt$$

$$= \frac{1}{W}\int_{\tau_\ell}^{\tau_\ell+W} i(t)dt + \frac{1}{W}\int_{\tau_\ell}^{\tau_\ell+W} i_n(t)dt - Ge\beta(P+k_n) \qquad (5)$$

where τ_ℓ represents the start of the loop integration; i.e., the timing of the loop. The subtraction in (5) represents the removal of the average intensity from the loop input. The dependence of the right-hand side on t is implicit in the parameter τ_ℓ, which varies as the loop attempts to track out the variations τ_d. Although τ_ℓ is actually a function of t it is treated as a constant when integrating over the pulse width W sec long. This latter fact is simply a restatement of the fact that the bandwidth of τ_ℓ, which is roughly the same as that of τ_d, is much less than the repetition frequency 1/W. After substituting the input processes, (5) can be rewritten as

$$e(t) = Ge\beta[N(\tau_\ell, \tau_\ell+W)/W + n - (P+k_n) \qquad (6)$$

where

$N(t_1, t_2)$ = number of photoelectrons occurring in the inverval (t_1, t_2)

n = Gaussian random circuit noise variable, having zero mean and variance $N_0/2W$, where N_0 is the one-sided circuit noise level.

The performance of the tracker can be directly related to the instantaneous timing error between the received and the oscillator signal. This timing error is defined by

$$\tau \triangleq \tau_d - \tau_\ell \tag{7}$$

where all parameters are actually functions of t. Using straightforward analog loop analysis, and recalling that the oscillator phase depends on the integral of the voltage controlling it, the timing error τ in (7) satisfies the integro-differential equation

$$\frac{d\tau}{dt} = \frac{d\tau_d}{dt} - Ke(t) \tag{8}$$

where K is the total loop gain. Since the error signal e(t) depends on both τ_d and τ_ℓ, the equation is in general non-linear in τ. Clearly, the solution for $\tau(t)$ in (8) necessarily evolves as a stochastic process due to the randomness of e(t) in (6). This is true even if the additive circuit noise $i_n(t)$ is set equal to zero (i.e., background limited operation) due to the randomness of the shot noise process.

Although the statistical properties of $\tau(t)$ will be of ultimate interest, the behavior of the instantaneous mean value of $\tau(t)$ can be derived from (8). If we statistically average both sides, interchanging differentiation and averaging on the left, we obtain the equation

$$\frac{d\bar{\tau}(t)}{dt} = \frac{d\bar{\tau}_1(t)}{dt} - K\overline{e(t)} \tag{9}$$

where the overbar denotes statistical average. Since the additive noise variable in (6) has zero mean, the mean error voltage is given by the mean shot noise count. The latter is the integrated count intensity over the integration intervals, as denoted by (4). Hence,

$$\begin{aligned}
\overline{e(t)} &= \mathcal{E}_\tau \left\{ \frac{Ge\beta}{W} \int_{\tau_\ell}^{\tau_\ell+W} I(t)dt - Ge\beta(P+k_n) \right\} \\
&= \mathcal{E}_\tau \left\{ \frac{Ge\beta}{W} \int_{\tau_\ell}^{\tau_\ell+W} \left[P\left[1 + p(t+\tau_1)\right]dt + k_n\right]dt - Ge\beta(P+k_n) \right\} \\
&= \mathcal{E}_\tau \left\{ \frac{e\beta GP}{W} \int_{\tau_\ell}^{\tau_\ell+W} p(t-\tau_\ell)dt \right\}
\end{aligned} \tag{10}$$

where $\mathcal{E}_\tau$ is the expectation operator over the random variable τ, and $p(t)$ is given in (2). The above integral can be rewritten in terms of a receiver correlation. Define the function $y(t)$ by

$$y(t) = \begin{cases} 1 & 0 \le t \le W \\ 0 & \text{elsewhere} \end{cases} \tag{11}$$

Then (10) becomes

$$\overline{e(t)} = \mathcal{E}_\tau \{e\beta GPR_{yp}(\tau)\} \tag{12}$$

where

$$R_{yp}(\tau_d - \tau_\ell) = \frac{1}{W} \int_{-\infty}^{\infty} p(t-\tau_d)y(t-\tau_\ell)dt \tag{13}$$

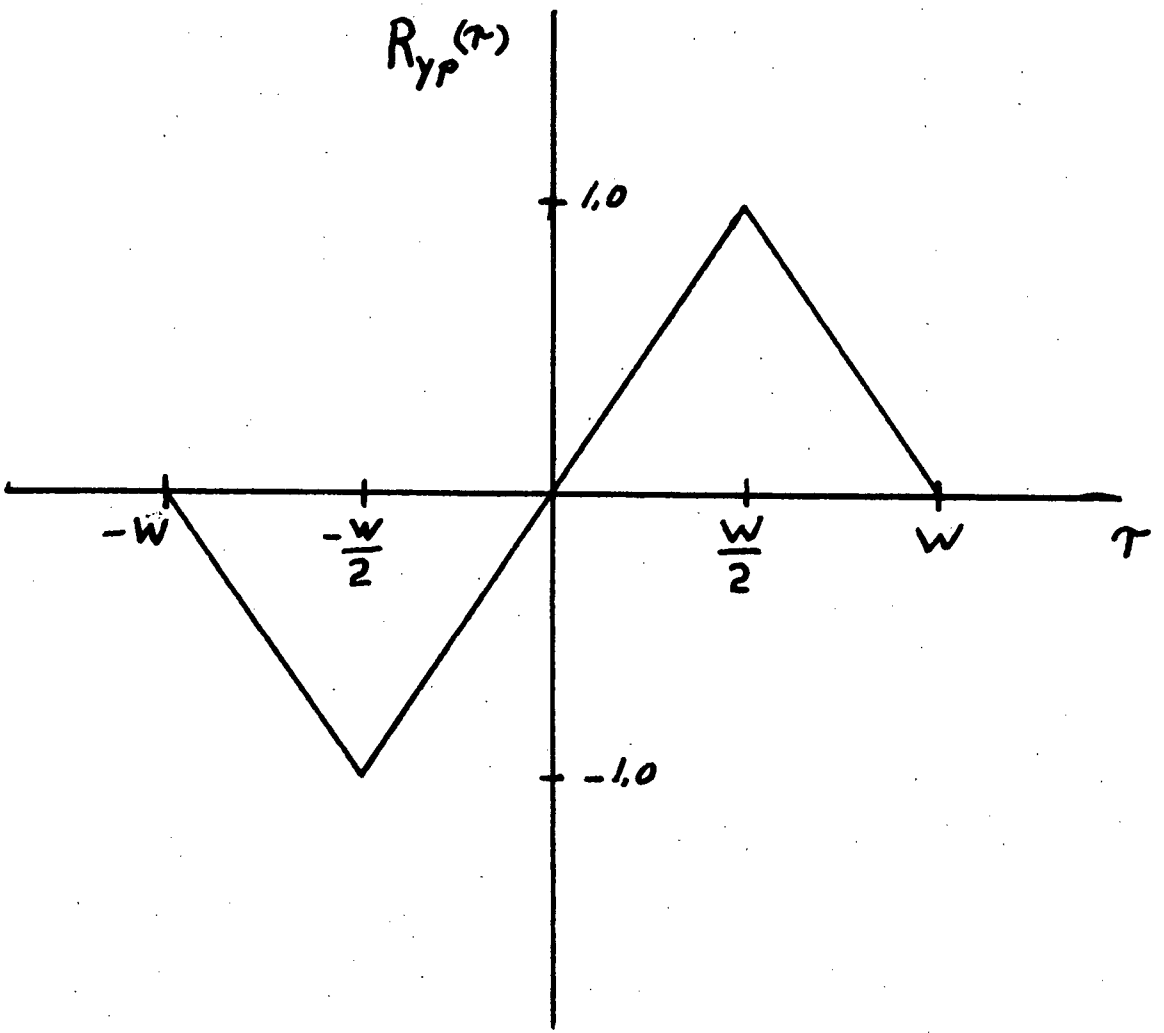

Figure 4

Hence, the mean of the error process can be related to the correlation of the periodic intensity modulation p(t) with the time function y(t). The latter function can therefore be considered as the receiver "timing" signal produced by the loop. The correlation function $R_{yp}(\tau)$ for the functions p(t) in (2) and y(t) in (11) is plotted in Figure 4. The latter can be considered as the mean error function of the tracking loop, and is often referred to as the loop "S curve".

Equation (9) therefore becomes

$$\frac{d\bar{\tau}(t)}{dt} = \frac{d\tau_l(t)}{dt} - (e\beta KGP)\delta_\tau\{R_{yp}(\tau)\} \qquad (14)$$

The above is the differential equation of the mean timing error variable in the tracking loop. If $\tau(t)$ is confined to the linear range of $R_{yp}(\tau)$ [i.e., if $\tau \approx 0$ and the loop is tracking well] then we can approximate $R_{yp}(\tau) \approx 2\tau/W$ and $\delta_\tau\{R_{yp}(\tau)\} \approx \delta_\tau\, 2\tau/W = 2\bar{\tau}/W$. Equation (14) then becomes a <u>linear</u> differential equation in terms of the mean error process $\bar{\tau}(t)$. Furthermore, this linear equation corresponds to that of the linear feedback system in Figure 5. The latter is often called the linear mean equivalent loop to Figure 3, and is useful for analyzing or synthesizing based upon the mean timing error process. Note that in this equivalent system, the input delay variation τ_d appears as the loop input, and the loop timing oscillator becomes a feedback loop integrator whose output is the timing process $\tau_\ell(t)$. The linear equivalent loop has a loop gain of $2eGK\beta P/W$ and a loop bandwidth* of

*In a linear feedback system, if H(S) is the transfer function from loop input to feedback signal, then the loop bandwidth is defined by $B_L = \int |H(j\omega)|^2 d\omega/2\pi$. It essentially represents the bandwidth that the loop exhibits to the input.

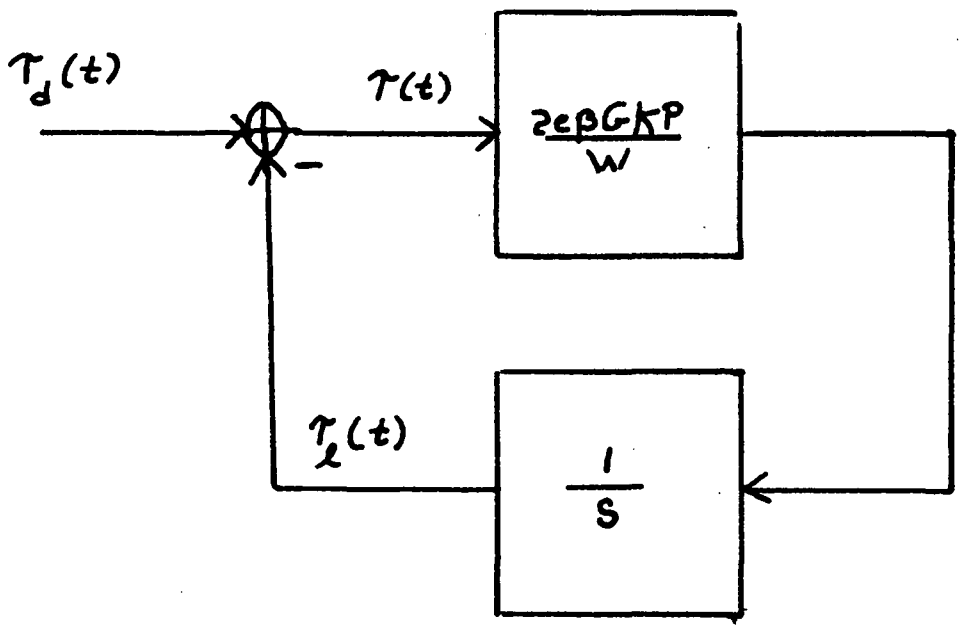

Figure 5

$$B_L = \frac{eGK\beta P}{2W} \tag{15}$$

Note that the loop bandwidth depends directly on the received optical power P, which therefore appears as a parameter of the equivalent system. The loop bandwidth must be sufficiently wide (i.e., there must be sufficient loop gain) to track the expected time variations in τ_d.

Although mean error performance in tracking the received delay variations can be determined from the linear mean system, the adverse effects due to the random nature of the optical field and circuit noise cannot be derived (note that the linear system is noiseless). In this case, the dynamical equation of the true system, Equation (8), must be examined in detail for a complete statistical analysis. The stochastic, non-linear nature of the timing error equation indicates that the statistics of the solution $\tau(t)$ will be highly non-stationary as the process evolves in time. An indication of the statistical properties of $\tau(t)$ can be obtained by examining the steady state probability density of τ/W. This latter density, $f(\tau)$, is known to satisfy the Kolmogorov-Smoluchowski steady state equation [5]:

$$\sum_{j=1}^{\infty} \frac{(-1)^j}{j!} \frac{\partial^{j-1}}{(\partial\tau)^{j-1}} \left[K_j(\tau) f(\tau)\right] = 0 , \quad |\tau| < 1 \tag{16}$$

where

$$K_j(\tau) = \lim_{\Delta t \to 0} \frac{\overline{(\Delta\tau)^j}}{\Delta t} \tag{17}$$

$$\Delta\tau = \left[\tau(t+\Delta t) - \tau(t)\right]/W$$

with the condition that $f(\tau)$ integrate to one. When the coefficients $K_j(\tau)$ exist, this equation provides a relation that must be satisfied by the steady state density of the process $\tau(t)$. The equation is a partial differential equation with variable coefficients and, in general, involves all orders of derivatives. The principle usefulness of (16), however, occurs when only the first few coefficients are non-zero. In particular, if $K_j(\tau) = 0$, $j \geq 3$ the resulting equation is the steady-state Fokker-Planck equation, and has been extensively studied [6]. A Fokker-Planck equation implies a "continuous" process; i.e., processes that do not change significantly over a short time period, while the more general equation of (16) would be associated with processes containing statistical jumps.

The calculation of the sequence of coefficients $K_j(\tau)$ requires determination of the moments of the error increment $\Delta\tau$ in (17). Consider again the system of (8) when tracking an intensity pulse having a constant time shift $\tau_d(t) = \tau_0$. The timing error $\tau(t)$ therefore satisfies (8) with $d\tau_d/dt = 0$. The timing error variation $\Delta\tau$ is then

$$\Delta\tau = \frac{1}{W}\int_t^{t+\Delta\tau}\left(\frac{d\tau}{dz}\right)dz$$

$$= -K/W\int_t^{t+\Delta\tau} e(z)dz \qquad (18)$$

The coefficients in (17) can now be determined by using (6) in (18). It is shown in Appendix A that these coefficients become

$$K_j(\tau) = \begin{cases} -(eGK\beta P)R_{yp}(\tau), & j = 1 \\ (GeK)^2[\beta R_{y^2I}(\tau) + N_0/2WGe]/W & j = 2 \\ (-eGK)^j[R_{y^jI}(\tau)]\beta, & j \geq 3 \end{cases} \tag{19}$$

where

$$R_{y^jI}(\tau) = \frac{1}{W}\int_{-\infty}^{\infty} y^j(t-\tau_\ell)I(t-\tau_d)dt \tag{20}$$

For the loop signal y(t) in (11), the above can be further simplified by noting that for all j

$$R_{y^jI}(\tau) = R_{yI}(\tau) = (P + k_n) + PR_{yp}(\tau) \tag{21}$$

Thus, the steady state Kolmogorov equation becomes

$$0 = (eGK\beta P)[R_{yp}(\tau)f(\tau)] + \frac{(eGK)^2}{2W}\frac{d}{d\tau}\{[\beta R_{yI}(\tau) + N_0/2GeW]f(\tau)\}$$

$$+ \sum_{j=3}^{\infty} \frac{(eGK)^j}{j!W^{j-1}}\frac{d^{j-1}}{d\tau^{j-1}}\{\beta R_{yI}(\tau)f(\tau)\} \tag{22}$$

The infinite number of derivatives manifests the jump nature of the error process caused by the input shot noise. Although an exact solution for $f(\tau)$ is somewhat ambitious, some meaningful information and approximating solutions can be derived. In particular, consider the case where the system operates in near-lock operation, so that it may be assumed that $\tau \approx 0$. The instantaneous tracking error can therefore be considered to be confined to the linear range of $R_{yp}(\tau)$ and, approximately,

$$R_{yp}(\tau) \approx 2\tau/W$$
$$R_{yI}(\tau) \approx (P + k_n) \tag{23}$$

Substituting into (22) and dividing by the coefficient of the second term yields the modified equation:

$$0 = -\alpha\tau f(\tau) + \frac{d}{d\tau} f(\tau) + \sum_{j=3}^{\infty} A_j \frac{d^{j-1}}{d\tau^{j-1}} f(\tau) \tag{24}$$

where

$$\alpha = \frac{\beta P}{eGK/2W\left[\beta(P+k_n) + N_0/2GeW\right]} \tag{25}$$

$$A_j = \frac{1}{j!}\left(\frac{-1}{\alpha}\right)^{j-2} \left[\frac{\beta(P+k_n)(\beta P)^{j-2}}{\left[\beta(P+k_n) + N_0/GeW\right]^{j-1}}\right] \tag{26}$$

Note that the coefficients A_j vary as $1/\alpha^{j-1}$, exhibiting a decreasing importance in the higher derivatives as the parameter α in (25) is increased. [The bracketed term in A_j is bounded by one and approaches one as the system approaches quantum limited operation, i.e., when $\beta P \gg \beta k_n + N_0/GeW$.] A physical interpretation to α can be introduced by using the linear mean-equivalent loop of Figure 5. Since it is desirous to operate the tracking loop with a given loop bandwidth B_L the loop gain K can be adjusted so as to obtain this value in (15). Hence $K = 2B_L/Ge\beta PW$, and (25) becomes

$$\alpha = \frac{(\beta P)^2}{2B_L\left[\beta(P+k_n) + N_0/WGe\right]} \tag{27}$$

When written in this way, the numerator is the square of the mean intensity of the received signal, while the denominator is effectively the total noise

power occurring in the bandwidth B_L (since the level $\beta(P+k_n)$ is the two-sided shot noise spectral level). Thus, α is essentially a signal to noise power ratio. Alternatively, (25) can be factored as

$$\alpha = \left[\frac{\beta P/2B_L}{1 + \frac{k_n}{P} + \frac{N_0/GeW}{\beta P}} \right] \tag{28}$$

Since the received power in a optical beam is equivalently the average rate of received photoelectrons, the numerator represents the average number of electrons produced in a $1/2B_L$ time period. In this way, α can be considered as a normalized photoelectron count density, indicating the accumulation of electron, over a time period equal to the reciprocal of the loop bandwidth. Furthermore the normalizing factor in the denominator becomes one for quantum-limited operation. Hence, coefficients A_j in (26) essentially vary inversely with the electron density of the received optical field.

Further properties of the solution for $f(\tau)$ for the in-lock operation case can be readily derived from (24). Transforming both sides indicates that the characteristic function of $f(\tau)$, $\varphi(\omega)$, satisfies the differential equation

$$-\alpha \frac{d\varphi(\omega)}{jd\omega} + j\omega\varphi(\omega) + \sum_{i=2}^{\infty} A_i (j\omega)^i \varphi(\omega) = 0 \tag{29}$$

This means

$$\ln \varphi(\omega) = -\frac{\omega^2}{2\alpha} + \frac{1}{\alpha} \sum_{i=2}^{\infty} \frac{A_i (j\omega)^{i+1}}{i+1} + C \tag{30}$$

where C is chosen to satisfy the unit area constant on $f(\tau)$. Since the left hand side is in the form of a power series in $j\omega$, the semi-invariants of the steady state density can immediately be identified. Note that the first semi-invariant (mean value) is zero, the second semi-invariant (variance) is $1/\alpha$, and the higher semi-invariants are related to the $\{A_i\}$. Thus, the actual form of the solution density depends on these coefficients. As a limiting case, however, we see that if $\alpha \to \infty$ implying $A_i/\alpha \to 0$ for all i, then $\ln \varphi(\omega) = -\omega^2/2\alpha$, corresponding to a zero mean, Gaussian density for τ, having variance $1/\alpha$. On the other hand, for $\alpha < \infty$ the higher coefficients can no longer be neglected, and the complete series in (30) must be included. In quantum limited operation, $A_i = (-\alpha)^{i-1}/i!$, and (26) has the closed form

$$\ln \varphi(\omega) = \alpha \left[e^{j(\omega/\alpha)} - 1 \right] - j\omega \qquad (31)$$

which means

$$\varphi(\omega) = \exp\left[\alpha e^{j(\omega/\alpha)} - 1\right] \exp\left[\alpha(j\omega/\alpha)\right] \qquad (32)$$

This can be recognized as the characteristic function of a linearly transformed Poisson variable with rate α. That is, (32) is the characteristic function of the random variable

$$\tau = \left(\frac{1}{\alpha}\right) x - 1 \qquad (33)$$

where x is a Poisson random variable with rate parameter α. This itself is a discrete variable, having zero mean, and takes on the values $1/\alpha$, $2/\alpha$, $\ldots n/\alpha$ with Poisson probability at each n. This means the loop is exhibiting the jump nature of the input shot noise process by linearly reproducing jumps

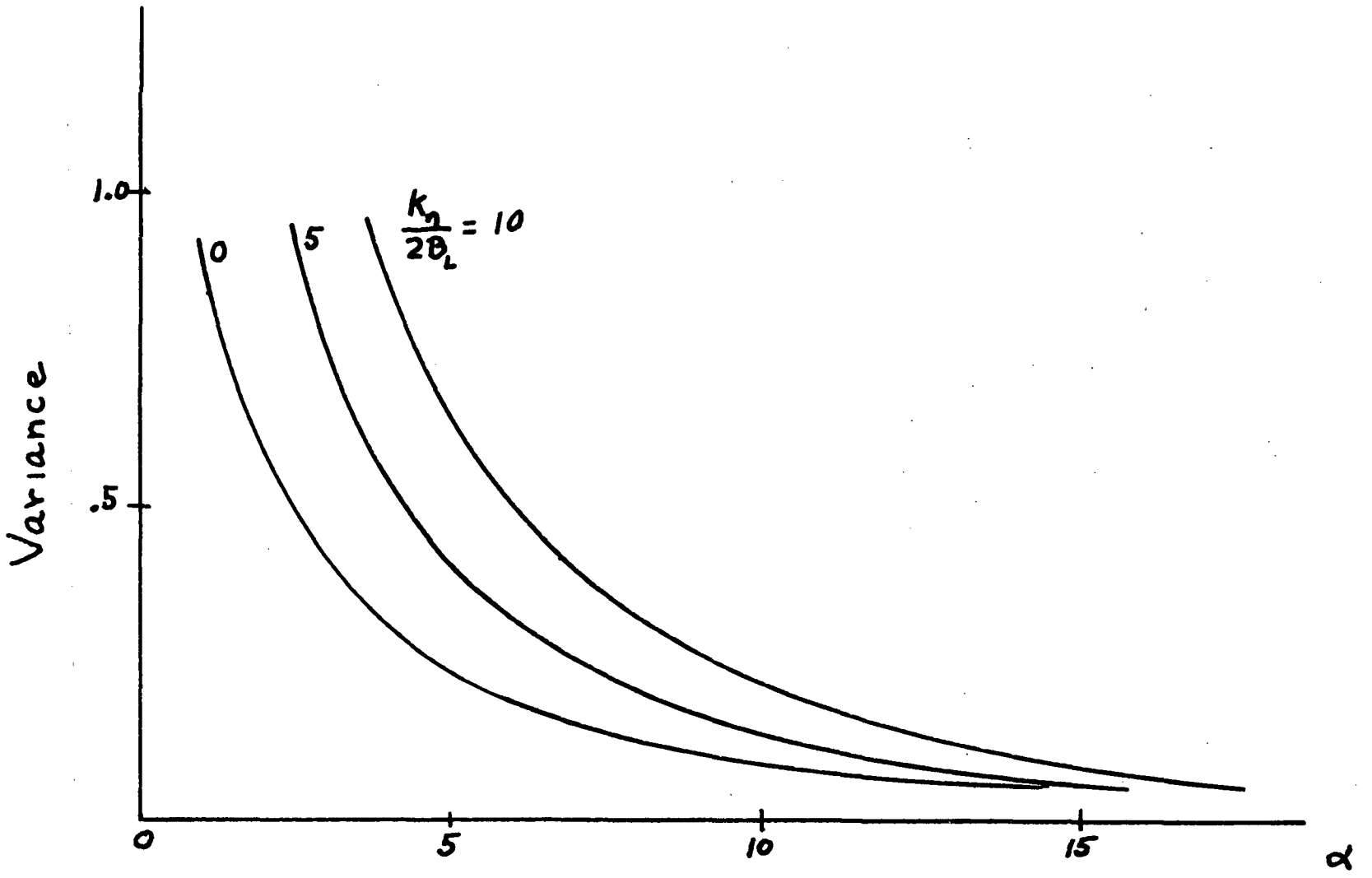

Figure 6

as the discrete arrivals occur. It must be remembered however that the above is based on a complete linear loop model. As α is decreased in value the size of the discrete loop error jumps (multiples of $1/\alpha$) will cause the loop error to exceed the linear range of $R_{yp}(\tau)$, violating our assumption that the loop is in fact completely linear. It is important to recognize nonetheless that as the loop error density varies in form from the asymptotic Gaussian density for $\alpha \to \infty$ to the modified discrete Poisson density for $\alpha \to 0$, the variance of the density is always $1/\alpha$ [i.e., the second semi-invariant in (30)]. The linear loop error variance, normalized to the pulse width W and assuming shot noise limited operation, is therefore

$$\sigma_\tau^2 = \frac{2B_L}{\beta P}\left[1 + \frac{k_n}{P}\right] \tag{34}$$

The above is plotted in Figure 6 as a function of the parameter $\alpha = \beta P/2B_L = P/hf2B_L$, for several values of normalized noise energy $k_n/2B_L$. The curves, in essence, summarize the performance of a pure sync system operating with optical power P watts in a tracking bandwidth of B_L hz. The rapid increase in the fractional error variance as the sync signal to quantum noise ratio is decreased represents the deterioration of the timing performance. The presence of background noise k_n causes the increase to occur at higher values of α. Recall again that α can be interpreted as the average number of signal photons received in the loop response time $1/2B_L$, while $k_n/2B_L$ has a similar interpretation in terms of noise photons.

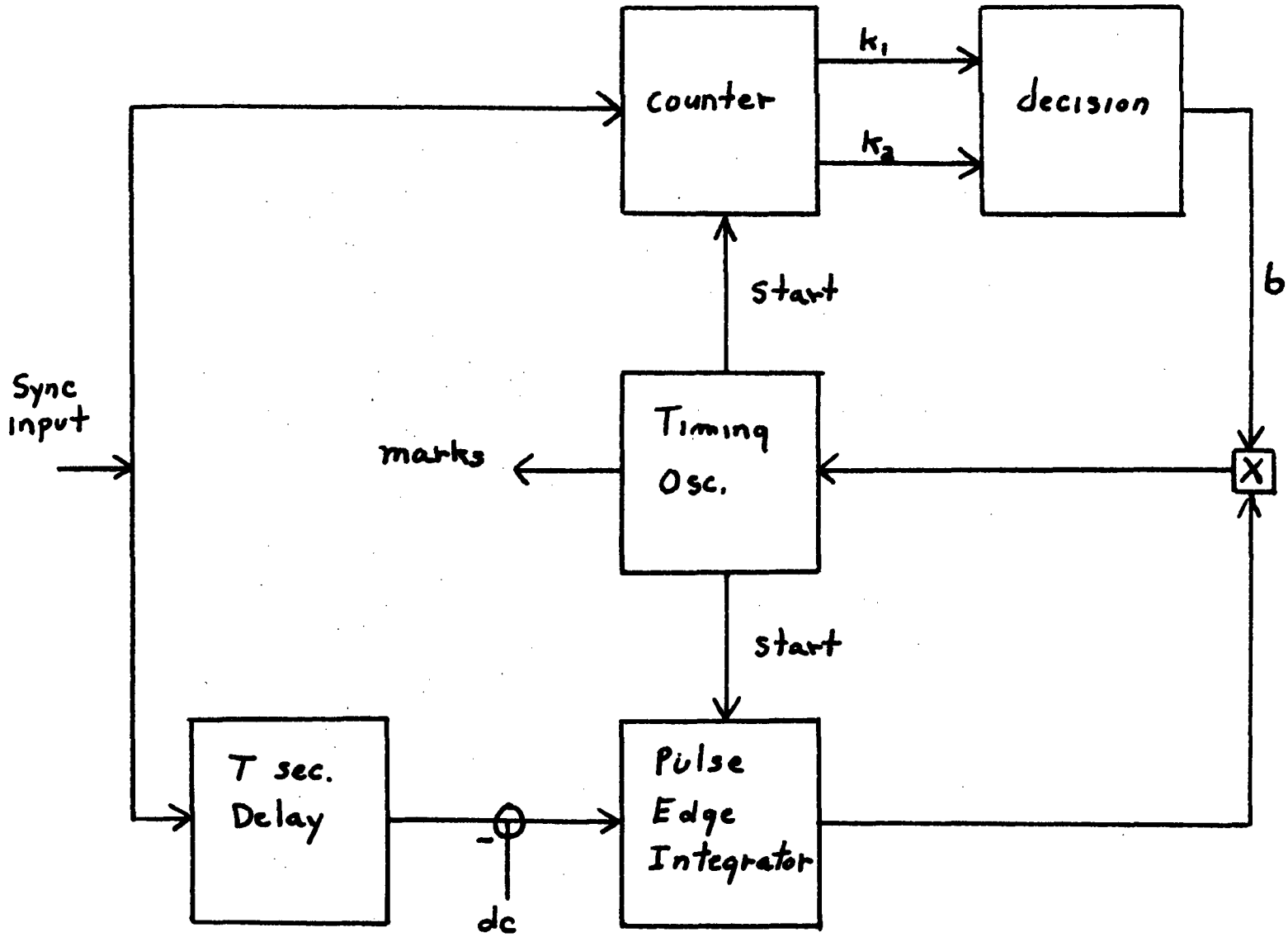
counter
k_1
k_2
decision
start
b
Sync input
marks
Timing Osc.
X
start
T sec. Delay
-
dc
Pulse Edge Integrator

Figure 7

4.0 Modulation-Derived Edge Tracking with PPM

In a PPM system the received optical intensity is no longer periodic, but varies in position according to the data bit sequence. For example, in binary PPM, if the optical intensity is written as in (1), then its modulation during a bit period is given by p(t) in (2) if a binary one is sent, but is given by -p(t) if a binary zero is sent, as obvious from Figure 2a. A receiver attempting to attain time synchronization by edge tracking the center transitions during each bit period will be adversely affected by the data modulation. If a data one is sent, a timing error τ will generate a loop error voltage of $R_{yp}(\tau)$, as discussed in Section 3. However, if a data zero is sent, an error voltage of $-R_{yp}(\tau)$ is generated in the same loop. Hence, for equally likely data bits, the average error voltage within the loop is then $[R_{yp}(\tau)$ (probability of one being sent)$-$ $R_{yp}(\tau)$ (probability of zero being sent)$] = 0$. That is, on the average, no loop error is generated for controlling the receiver timing oscillator during modulation reception.

To compensate for this modulation, an augmented edge tracking system is used, as shown in Figure 7. The decision loop attemps to determine the true data bit, using this result to properly modify the sign of the loop error voltage. This can be implemented by multiplying the generated error in a delayed (by one bit period) tracking loop by a plus or minus one, depending on the data bit. This latter decision is made from a count comparison over

each possible bit subinterval as they arrive. Thus, the error in the delayed edge-tracking loop becomes be(t), where

$$b = \begin{cases} +1 & \text{if one is sent} \\ -1 & \text{if zero is sent} \end{cases} \tag{35}$$

or equivalently,

$$b = \begin{cases} +1 & \text{if } k_1 \geq k_2 \\ -1 & \text{if } k_1 < k_2 \end{cases} \tag{36}$$

where k_1, k_2 are the counts over the first and second subinterval of each bit period. The differential equation in (8) for the tracking loop error now becomes

$$\frac{d\tau}{dt} = \frac{d\tau_1}{dt} - K[be(t)] \tag{37}$$

Since the counts in (36) are random counts, the parameter b is a random variable. Thus, the coefficients $K_j(\tau)$ in (17) for the steady state density will be a function of this variable, and therefore require a subsequent average over its statistics. When a one is sent the probability that $k_1 \geq k_2$ is equivalent to the probability that the one is correctly detected, whereas the probability that $k_1 < k_2$ corresponds to the probability that an error is made. Hence, when a one is sent,

$$b = \left\{ \begin{matrix} +1 & \text{with probability } 1-PE_1 \\ -1 & \text{with probability } PE_1 \end{matrix} \right\} \tag{38}$$

where PE_1 is the bit error probability when a one is sent. When a zero is sent, the above signs are reversed and PE_1 is replaced by PE_0. It

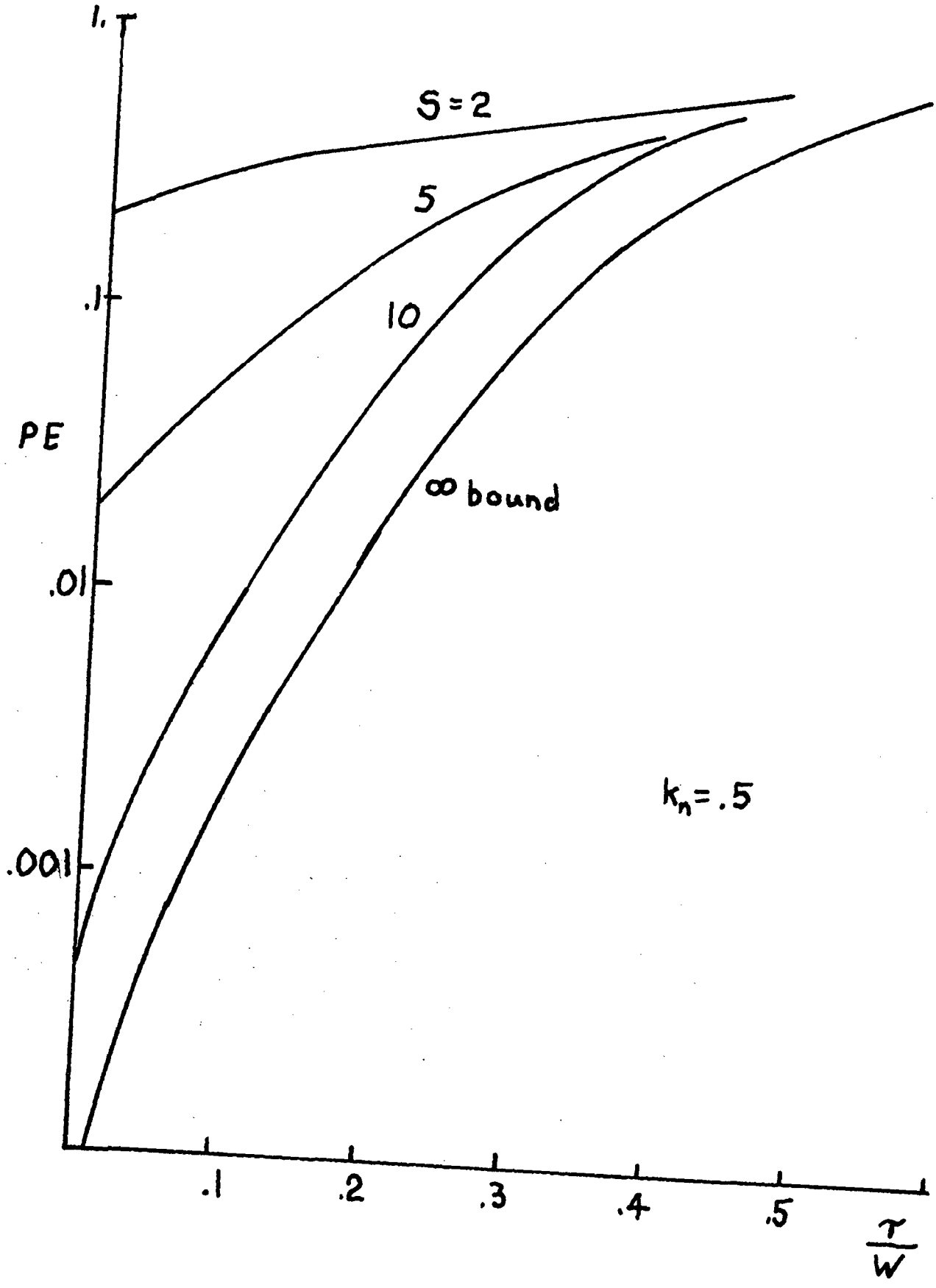

Figure 8

should be remembered, however, that the timing for this subinterval counting is in turn controlled by the receiver loop timing signal, which will have loop timing errors incorporated within it. Thus, the bit error probabilities in (38) must include these timing error effects. [A timing error between the true bit arrival time and the start of subinterval counting will cause the counting to occur over an offset interval.] The effect of these timing errors on bit decisioning has been previously derived, [2], and a typical average bit error probability plot of $PE = \frac{1}{2}[PE_1 + PE_0]$ is shown in Figure 8, as a function of the timing error τ and optical signal and noise powers. This timing error τ is in fact a function of time, but can be considered a constant over several bit periods.

The steady state coefficients $K_j(\tau)$ can be evaluated from (17), (19) and (37), first conditioning on b, then averaging over the probabilities in (38). Using primes to denote the K_j coefficients when data modulation is present, and noting that $b^j = 1$ for all j even, we see that

$$K'_j(\tau) = \begin{cases} K_j(\tau), & j \text{ even} \\ \frac{1}{2}K_j(\tau)\{(+1)[1-PE_1] + (-1)PE_1(\tau) - (-1)[1-PE_0] \\ \qquad - (+1)PE_0\}, & j \text{ odd} \end{cases}$$

$$= \begin{cases} K_j(\tau), & j \text{ even} \\ K_j(\tau)[1-2PE(\tau)], & j \text{ odd} \end{cases} \qquad (39)$$

where $PE(\tau) = \frac{1}{2}[PE_1 + PE_0]$. Note that the dependence of PE on τ has been emphasized. The resulting steady state density equation is again given by (16)

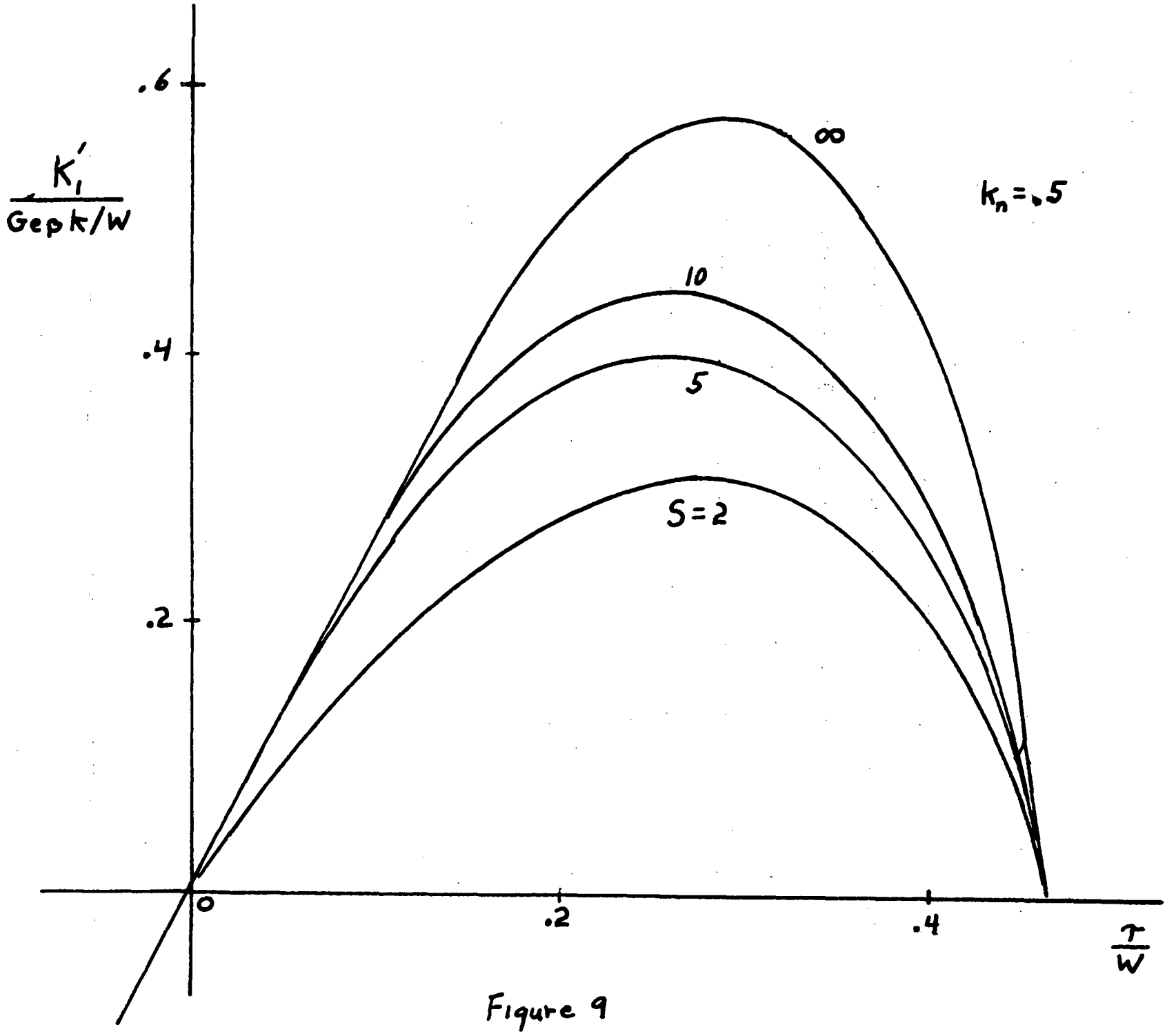

Figure 9

with $K_j(\tau)$ replaced by the $K_j'(\tau)$ above. Note that the coefficients are now more complicated functions of τ due to the auxiliary decisioning, and approach the earlier results as $PE(\tau) \to 0$. In this latter case, the system is correctly identifying the true bit during each period, and essentially "removing" the binary modulation. The first coefficient, $K_1'(\tau) = GEK\rho PR_{yp}(\tau)[1-2PE(\tau)]$, is the average loop error function, and represents the modified nonlinearity of the mean equivalent loop, as in (12). This coefficient is plotted in Figure 9 as a function of the normalized τ and received pulse energy S, obtained by use of Figures 4 and 8. Note that the effect of the decision process is to reduce the width and amplitude of the tracking error function. As $PE(\tau) \to \frac{1}{2}$, there is no average error being generated for loop tracking, and the system essentially loses lock.

For the near-lock assumption [use of (23)] the previous steady state equation is modified to

$$0 = -\alpha\tau[1-2PE(\tau)]f(\tau) + \frac{df(\tau)}{d\tau} + \sum_{j=3}^{\infty} A_j \frac{d^{j-1}}{d\tau^{j-1}} f(\tau) \qquad (40)$$

with $|\tau| \leq 1$. Even with this simplification, neither the solution density nor its characteristic function, can be generated as easily as in Section 3, since the first coefficient is now more complicated. However, the fractional variance for this density can be estimated by approximating the coefficient $K_1'(\tau)$ in Figure 9 by a sinusoid of proper amplitude and frequency. This latter amplitude will depend on the energy S per data bit used for decreasing, which in turn is related to the α parameter in

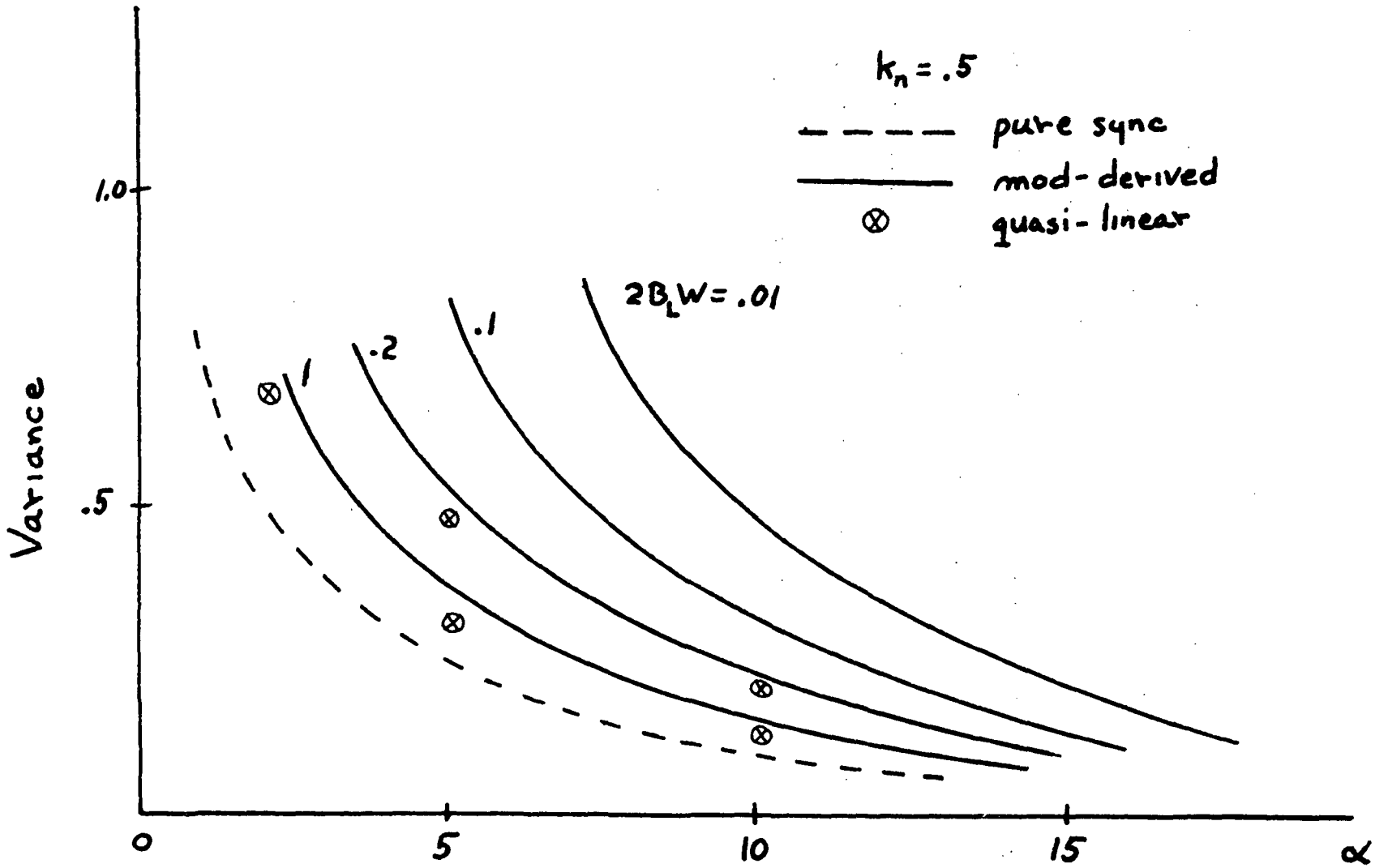
$k_n = .5$
pure sync
mod-derived
quasi-linear
$2B_LW = .01$
.1
.2
1
Variance
1.0
.5
0
5
10
15
α

Figure 10

(27) by

$$S = (2B_L W)\alpha \tag{41}$$

where $2B_L W = 2B_L/2R_b = B_L/R_b$. The latter parameter is the ratio of tracking loop bandwidth to the data bit rate R_b, and is typically less than one. When written as in (41), $2B_L W$ can also be interpreted as the fraction of the sync energy α appearing in the data pulse and therefore used in the auxiliary decisioning. For a fixed value of $2B_L W$, each value of α generates a corresponding value of S, to which an effective one cycle sin wave can be filtered to the corresponding curves of $K_1'(\tau)$ as in Figure 9. The variance can then be determined at each α by numerically solving a truncated version of (40), using the method discussed in Appendix B. The resulting normalized variance computed in this way is plotted in Figure (10), as a function of α for several values of $2B_L W$. The curve for the noiseless, pure sync operation from Figure 6 is superimposed. The results show that a deterioration of performance occurs over pure sync, due to the decisioning process, and can therefore be considered as the price to be paid for modulation derived synchronization. Note that the decisioning causes system degradation similar to an effective loss in signal to noise ratio (reduced α) and can therefore be interpreted as a power loss in the sync subsystem.

Although the use of the curves in Figure 10 are convenient for assessing performance, their derivation requires a somewhat lengthly calculation. Furthermore, this computation must be repeated at each desired value

background noise k_n. However a simpler method can be used, at the expense of analytical accuracy, to derive similar curves. This method makes use of a form of truncated quasi-linear solution, which bascially amounts to reducing (40) to a second order equation, and replacing the first coefficient by a modified linear coefficient as in (24), but retaining its dependence on the decision error probability PE. To accomplish this linearization we first recognize that PE depends on both pulse energy S, and timing error τ, and we write this as $PE(S,\tau)$. To linearize, we replace the functional dependence on τ by the root mean square value of τ; i.e., $\tau_{rms} = \sqrt{1/\alpha}$. Thus, using (41), we consider $PE(2B_L W\alpha, \sqrt{1/\alpha})$. The quasilinear differential equation for the timing error density $f(\tau)$ is then taken as

$$\frac{df(\tau)}{d\tau} - \alpha\left[1-2PE(2B_L W\alpha, \sqrt{1/\alpha})\right]\tau f(\tau) = 0 \qquad (42)$$

Note the equation is linear in τ, but the coefficients are nonlinear in α. The solution for $f(\tau)$ in (42) yields a Gaussian density with variance

$$\text{Variance} = \frac{1}{\alpha\left[1-PE(2B_L W\alpha, \sqrt{1/\alpha})\right]} \qquad (43)$$

The values of PE at any value of α and $B_L W$ can be obtained from curves similar to Figure 8. Several points of the above variance are superimposed in Figure 10. The results tends to display the same behavior for tracking performance, although the variance values indicate slightly lower variances than the more accurate results determined earlier.

ACKNOWLEDGEMENT

The author is grateful to Mr. Ronald Papa for his help in the computer calculations used throughout the paper.

APPENDIX A

The coefficients in (17) can be computed as a time average of the moments of the statistical variations in (18), neglecting the short term integration within the loop. Using i(t) as given in (3), and substituting y(t) from (11), yields

$$\begin{aligned}\Delta\tau &= \int_t^{t+\Delta t}\left[C\sum_m^{k_1}\delta(z-t_m) + Ki_n(z)/W - C\beta(P+K_n)\right]dz \\ &= \int_t^{t+\Delta t}\left[Cy(z-\tau_\ell)\sum_m^{k_1}\delta(z-t_m) + Ki_n(z)/W\right]dz - C\beta(P+K_n)\Delta t \\ &= C\sum_m^{k_2} y(t_m-\tau_\ell) + \frac{K}{W}\int_t^{t+\Delta t} i_n(z)dz - C\beta(P+K_n)\Delta t \qquad (A\text{-}1)\end{aligned}$$

where $C = GeK/W$, $k_1 = k(\tau_\ell, \tau_\ell+W)$, and $k_2 = k(t, t+\Delta t)$, the latter defined in (6). To determine the K_j coefficients the moments of $\Delta\tau$ must be calculated. The first two moments are as follows

$$\overline{[\Delta\tau]} = C\left[\overline{\sum_m^{k_2} y(t_m-\tau_\ell)}\right] + \frac{K}{W}\int_t^{t+\Delta t}\overline{[i_n(z)]}dz - C\beta(P+K_n)\Delta t \qquad (A\text{-}2)$$

Now $\overline{i_n(z)} = 0$ and it is known that Poisson shot noise has mean [4, pp. 1619]

$$\overline{\sum_m^{k_2} y(t_m-\tau_\ell)} = \beta\int_t^{t+\Delta t} y(t_m-\tau_\ell)I(t_m-\tau_d)dt_m \qquad (A\text{-}3)$$

In the limit as $\Delta t \to 0$,

$$\lim_{\Delta t \to 0} \int_{t}^{t+\Delta t} y(a-\tau_\ell) I(a-\tau_d)\,da \to (\Delta t)\, y(t-\tau_\ell) I(t-\tau_d) \qquad \text{(A-4)}$$

It then follows that the time averaged first coefficient in (17) is

$$K_1 = \lim_{\Delta t \to 0} \frac{\epsilon(\Delta\tau)}{\Delta t} = C\beta \int_{-\infty}^{\infty} y(t-\tau_\ell) I(t-\tau_d)\,dt - C\Delta t P\beta$$

$$= C\beta \int_{-\infty}^{\infty} y(t-\tau_\ell)[I(t-\tau_d) - P]\,dt \qquad \text{(A-5)}$$

The calculation of the mean squared value of (A-1) requires computation of the cross products involved. However, noting that the eventual computation of the K_j requires a division by Δt followed by a limit as $\Delta t \to 0$, only the terms of order Δt need be retained. In particular, we see from (A-4) that any product of averages of the shot noise summation will always be at least of order Δt^2. Hence, we have

$$\overline{\epsilon(\Delta\tau)^2} = C^2 \left[\overline{\sum_{m}^{k_2} y^2(t_m - \tau_\ell)} \right] + \left(\frac{K}{W}\right)^2 \int_{t}^{t+\Delta t} \overline{i_n(z_1) i_n(z_2)}\,dz_1\,dz_2 + O(\Delta t^2) \qquad \text{(A-6)}$$

The average of the first summation is known to be [4, pp. 1619]

$$C^2\beta \int_{t}^{t+\Delta t} y^2(t_m - \tau_\ell) I(t_m - \tau_d)\,dt_m + 0(\Delta t^2) \qquad \text{(A-7)}$$

Since the circuit noise is white with spectral level N_0, the second integral is known to be $K^2 N_0 \Delta t/2W$ [7, pp. 86]. Proceeding as in (A-4), we have

$$K_2 = C^2\beta \int_{\infty}^{\infty} y^2(t-\tau_\ell) I(t-\tau_d)\,dt + \frac{K^2 N_0}{2W^2} \qquad \text{(A-8)}$$

Similarly, we have

$$\overline{(\Delta t)^j} = C^j \left[\overline{\sum^{k_2} y^j(t_m - \tau_\ell)} \right] + O(\Delta t)^2, \quad j \geq 3 \qquad (A\text{-}9)$$

By manipulating as above we finally derive

$$K_j = C^j \beta \int_{-\infty}^{\infty} y^j(t-\tau_\ell) I(t-\tau_d) dt$$

Equations (A-6), (A-8), and (A-9) are summarized in (19) of the paper.

APPENDIX B

Consider the equation

$$0 = [\alpha Q \sin 2\pi\tau] f(\tau) + \frac{df}{d\tau} + \sum_{j=3}^{N} A_j \frac{d^{j-1} f(\tau)}{d\tau^j} , \quad |\tau| \leq 1/2$$

$$A_j = \frac{1}{j!\alpha^j} \tag{B-1}$$

which is a truncated version of (40) with $K_1'(\tau) = Q \sin 2\pi\tau$. We assume an even solution having the form

$$f(\tau) = \sum_{k=0}^{\infty} C_k \cos 2\pi k\tau , \quad |\tau| \leq 1/2 \tag{B-2}$$

where

$$C_k = \int_{-\frac{1}{2}}^{\frac{1}{2}} f(\tau) \cos 2\pi k\tau d\tau \tag{B-3}$$

If we substitute (B-2) into (B-1), collect harmonic terms, set the resulting coefficients equal to zero, we derive the following second order recursive equations among the C_k:

$$C_{k+1} = C_{k-1} + \left[-\frac{2k}{Q\alpha} + \sum_{\substack{j=3 \\ (\text{odd})}}^{N} \frac{2A_j k^j}{Q\alpha} \right] C_k \tag{B-4}$$

The above allows a generation of all subsequent C_k from the first two, C_0 and C_1. These latter two are found from the conditions that 1) $f(\tau)$ be a probability density over $(-\frac{1}{2}, \frac{1}{2})$ and 2) for large α, $f(\tau)$ must approach the known solution corresponding to $A_j = 0$ in (40). From (B-3) we see that the first condition requires that $C_0 = 1$, while for $A_j = 0$, (B-4) becomes

$$C_{k+1} = C_{k-1} - \left(\frac{2k}{Q\alpha}\right) C_k , \quad C_0 = 1 \tag{B-5}$$

The solution is then

$$C_k = \frac{I_k(Q\alpha)}{I_0(Q\alpha)} \tag{B-6}$$

for all k. Thus, C_1 was selected as $I_1(Q\alpha)/I_0(Q\alpha)$ in subsequent analysis using (B-4). The density $f(\tau)$ can now theoretically be constructed by solving (B-4) and using the C_k in (B-2).

We are primarily interested in the variance of this tracking error, given by

$$\begin{aligned}
\sigma_\tau^2 &= \int_{-\frac{1}{2}}^{\frac{1}{2}} \tau^2 f(\tau) d\tau \\
&= \frac{C_0}{12} + \sum_{k=1}^{\infty} C_k \int_{-\frac{1}{2}}^{\frac{1}{2}} \tau^2 \cos 2\pi k\sigma d\tau \\
&= \frac{C_0}{12} + \sum_{k=1}^{\infty} C_k \left[\frac{(-1)^k}{2\pi^2 k^2}\right]
\end{aligned} \tag{B-7}$$

The above can be computed directly from the C_k generated from (B-4). To examine the truncation error (B-4) was numerically solved for Q in the range (.1-.5) and N = 0, 3 and 5. For the range of interest ($1 \leq \alpha \leq 100$) no noticeable change in variance appeared for N greater than 3. Hence, the truncation was limited to N = 3 in all subsequent results. With N = 3, the variance was then computed from (B-7) as a function of α, after generation of the C_k from (B-4). The value of Q, which itself depends on α, was determined for each α from the curves of Figure 9. The resulting variance is plotted in Figure 10 of the paper.

REFERENCES

[1] Karp, S. and Gagliardi, R., "The Design of PPM Optical Communication Systems," IEEE Trans. on Comm. Tech., Vol. COM-17, pp. 670, December, 1969.

[2] Gagliardi, R. M., "The Effect of Timing Errors in Optical Digital Systems," IEEE Trans. on Communications, Vol. COM-20, No. 2, pp. 87, April, 1972.

[3] Lindsey, W. C., and Simon, M., "Data-Aided Carrier Tracking Loops," IEEE Trans. on Comm. Tech., Vol. COM-19, pp. 157, April, 1971.

[4] Karp, S., et. al., "Communication Theory for the Free Space Optical Channel," Proc. of the IEEE, Vol. 58, No. 10, pp. 1611, October, 1970.

[5] Lindsey, W. C., Synchronization Systems in Communications and Control, (book) Prentice-Hall, 1971, Chapter 7.

[6] _____, Synchronization Systems in Communications and Control, loc. cit., Chapter 9.

[7] Viterbi, A., Principles of Coherent Communications, (book), McGraw-Hill, 1966.

FIGURE CAPTIONS

1. An optical digital PPM receiver
2. Intensity waveforms. a) PPM bit intensities, b) pure sync intensity
3. Pulse-edge tracking subsystem
4. Tracking error characteristic for pure sync
5. Linear equivalent edge-tracking loop
6. Variance of normalized error τ/W vs. loop SNR α (pure sync)
7. Modified edge tracking loop for PPM sync
8. Error probability curves vs. offset timing error
9. Modified loop error characteristic for PPM sync
10. Variance of normalized error vs. loop SNR α (PPM sync)


USC
Engineering